CHEMISTRY
AN ASIAN JOURNAL
www.chemasianj.org

Accepted Article

Title: A multi-stimuli-responsive oxazine molecular switch: A new strategy for the design of electrochromic materials

Authors: Xiaojun Wang, Chang Gu, Hongzhi Zheng, Yu-Mo Zhang, and Sean Xiao-An Zhang

To be cited as: *Chem. Asian J.* 10.1002/asia.201800282

Link to VoR: http://dx.doi.org/10.1002/asia.201800282

A Journal of
ACES
Asian Chemical Editorial Society

A sister journal of Angewandte Chemie and Chemistry – A European Journal

WILEY-VCH

A multi-stimuli-responsive oxazine molecular switch: A new strategy for the design of electrochromic materials

Xiaojun Wang, Chang Gu, Hongzhi Zheng, Yu-Mo Zhang* and Sean Xiao-An Zhang*

Abstract: A multi-state and multi-stimuli-responsive oxazine molecular switch combining electro-base property and sensitively base/acid responsive properties was designed and synthesized. The multi-state structures of the molecular switch with different colors were speculated by comparison the optical properties with reference molecules and confirmed by NMR. The color switching mechanism under the stimulation of acid and base was investigated by DFT calculation. Three single states can be obtained and the switching is unidirectional under the stimulation of acid and base. The electrochromic phenomenon of the molecular switch was demonstrated combining its electro-base property and base-sensitive property. An electrochromic device was successfully constructed which exhibits good electrochromic properties with excellent reversibility (2000 cycles) and high coloration efficiency (804 cm^2/C).

Introduction

Electrochromic materials (ECM), characterized by the tunable color being switched by electrical field,[1,2] have been attracting much attention in the past few decades due to their wide application potential,[3] such as smart windows,[4-7] auto rearview mirrors, reflect displays,[8-10] etc.[1,11] At present, metal oxides (WO_3),[5,11] conducted polymers[12-14] and viologen derivatives[15] are the three most intensively researched kinds of ECM. Even though all these materials exhibit unique advantages and attractive application potential in electrochromic devices, for example good photostability of WO_3, high color efficiency of conducted polymer and high reversibility of viologen.[13,16,17] There are still many problems such as slow response speed and difficult manufacturing processes for WO_3, few color choices for viologen, and poor color purity for conducted polymer.[16,18-20] Many efforts have been made to solve these problems.[18,21-25] And one promising way to solve these problems is exploiting new electrochromic materials.[26-33]

Molecular switches represent a kind of molecule whose properties such as optical properties, polarity and solubility can be changed when the structure of the molecule undergoes transformation under external stimuli such as light, heat, pH, force and electric field etc.[34-38] Among them, the pH-sensitive molecular switches are most abundant and have wide application in pH indicator, biosensing,[39] information communication etc.[40,41] More importantly, color of pH-sensitive molecular switches exhibits wide variety, high purity, and ideal molar absorption coefficient. However, the application of pH-sensitive molecular switches in ECM is hindered for the lack of ability of the electrical response.[42-44] The ‘‘electro-acid/base” was utilized by our group to extend the application of pH-sensitive molecular switches into ECM.[45-47] Electro-acid/base is a type of molecule (such as p-phenylenediamine and benzoquinone, etc.) which oxidative or reductive state exhibits capable of capturing/losing a proton. Compared with chemical acid/base, the acidity/alkalinity of electro-acid/base could be controlled by an external electric field in a closed system. Through utilizing these electro-acid/base molecules, various pH-sensitive molecular switches have the opportunity to application in ECM.

In this paper, a oxazine derivate (M−c, Figure 1a) was designed and synthesized. First, its pH-sensitive properties were studied systematically with a dual response to acid and base, and the structures of different states were speculated by comparing the optical properties with reference molecules and confirmed by NMR. The switching mechanism of M−c under the stimulation of acid/base was analyzed by DFT calculation. Then, the electro-base mechanism of M−c was demonstrated, and an electrochromic device was fabricated with good electrochromic properties.

Results and Discussion

The acid/base-responsive measurement in solution. The molecule M−c was designed by combining an acid responsive heterocyclic ring and a base responsive hydroxyl. And two reference molecules, M−r−1 and M−r−2, were also synthesized with similar structure with M-c as shown in Figure 1a. To investigate if the molecule M−c has the acid and base responsive properties respectively, the UV−vis absorption spectra of M−c with the addition of acid and base were measured. As shown in Figure 1b, with increasing concentration of the trifluoroacetic acid (TFA), the original absorption peak at 267 nm decreases, and a new absorption band at 436 nm emerges and increases. Only 0.5 equiv of the TFA was needed to stimulate its structural alteration. And it can be transformed into acid-form (M−a−o) completely under 5.0 equiv of TFA. Which demonstrate the M−c has good acid sensitivity. The M−c molecule still possessed good acid responsive reversibility. The absorption peak at 436 nm of M−a−o disappears immediately by adding the same amount of potassium tert-butoxide (t-BuOK) to neutralize the acid.

X. Wang, C. Gu, H. Zheng, Dr. Y. M. Zhang and Prof. S. X. A. Zhang
State Key Lab of Supramolecular Structure and Materials, College of Chemistry
Jilin University
2699 Qianjin Street, Changchun 130012, P. R. China.
E-mail: zhangyumo@jlu.edu.cn and seanzhang@jlu.edu.cn

Supporting information for this article is given via a link at the end of the document.

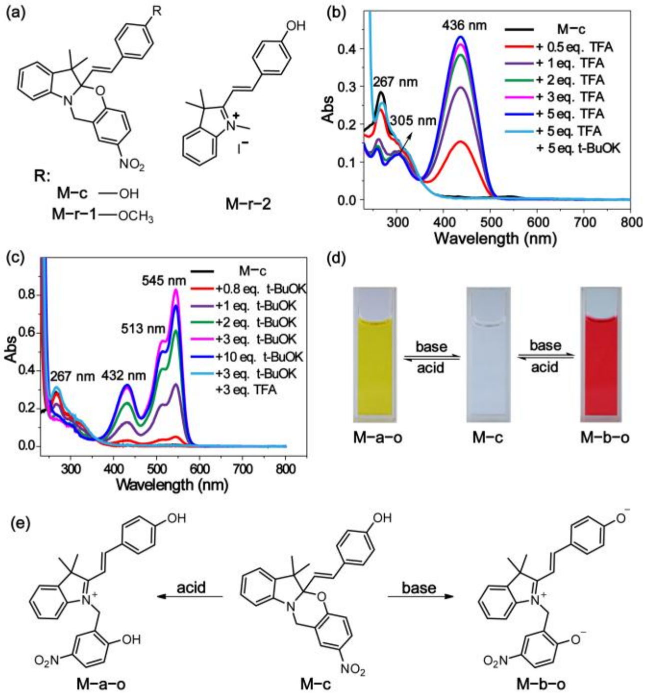

Figure 1. (a) The chemical structures of M−c molecule and the reference molecules, M−r−1 and M−r−2. (b) UV−vis absorption spectra of M−c (1.0×10^{-5} M) in acetonitrile, adding different equiv TFA, then neutralizing with t-BuOK. (c) UV−vis absorption spectra of M−c (1.0×10^{-5} M) in acetonitrile, adding different equiv t-BuOK, then neutralizing with TFA. (d) The color changing pictures for M−c solution in acetonitrile stimulated reversibly by the acid and base. (e) The structure speculation for the acid-form and base-form of M−c.

The base measurement is shown in Figure 1c. With increasing base concentration, the absorption peak at 267 nm decreases, and the absorption peaks at 432 nm, 513 nm and 545 nm increase. Just 3.0 equiv t-BuOK was needed to achieve the maximum absorbance peak at 545 nm, along with transforming M−c to base form (M−b−o) completely. Which indicates the M−c molecule with good base sensitivity. And then adding 3.0 equiv TFA to neutralize the t-BuOK, the absorption spectrum recover to the initial state. This measurement declares that M-c also has base-responsive reversibility. The pictures of acid/base stimulated solutions were shown in Figure 1d, with yellow color in acid-form M−a−o, colorless in neutral state M−c and red color in base-form M−b−o.

According to the literature, this heterocyclic ring structure will be changed to open form after stimulated by the acid.[43] The structure of the open form is speculated as M−a−o (Figure 1e). M−r−1 with methoxyl exhibits the similar acid responsive property with M−c as shown in Figure S1, which indicates that the acid responsive behavior of M−c is dependent on the heterocyclic ring, not hydroxyl. Refer to the absorption peak at 424 nm of M−r−2 (Figure S2) and the absorption peak at 306 nm for p-nitrophenol (Figure S3), the emerged absorption peak at 436 nm in Figure 1b is supposed to come from the conjugated part of the M−a−o, which is same with the structure of M−r−2. And the absorption peak at 305 nm can be assigned as the absorption of nitrophenol group. 12 nm red shifts between the absorption peaks of M−c−o and M−r−2 may be due to the spatial electron dipole on the p-nitrophenol as a non-conjugated substituent.

To understand the structural change of M−c in base-treating process, base responsive properties of M−r−1, M−r−2 and p-nitrophenol were also investigated. For the M−r−1, there is no change of the UV-vis spectrum after adding 5 equiv t-BuOK as shown in Figure S4. It declares that the hydroxyl group is the important functional group for M−c molecule. The base responsive properties of M−r−2 are studied as shown in Figure S2. With the concentration of t-BuOK increasing, the absorption peak at 424 nm decreases to zero, and the absorption peaks at 538 nm and 507 nm increase. Those peaks are similar with the absorption peaks at 545 nm and 513 nm for the M−c molecule, and only 7 nm and 8 nm differences are exhibited. It demonstrates that the base form of M−c has similar structure with the base form of M−r−2. Hereinto, the hydroxyl of M−r−2 is changed to oxygen anion after t-BuOK being added, which can be proposed readily (Scheme S1a). Only 3 nm difference was exhibited between the absorption peaks for 432 nm of base-form M−c and 429 nm of base-form p-nitrophenol (Figure S3). Therefore, after stimulated by t-BuOK, the M−c molecule should undergo a proton loss, and then the ring-opening process of heterocyclic ring to generate a large conjugated part as shown as M−b−o in Figure 1e, similar to base form of M−r−2. A 109 nm red shift of the absorption peak position from 436 nm (M−a−o) to 545 nm (M−b−o) is produced by the property of the oxygen anion as stronger electron donor compared with hydroxyl. The absorption peaks of 545 nm and 513 nm are supposed to come from trans-cis isomerism of the double bond on the conjugated part. Furthermore, molar absorption coefficients of M−b−o (545 nm, $\varepsilon=9.677\times10^{4}$ $L{\cdot}mol^{-1}{\cdot}cm^{-1}$) is also obviously higher than M−a−o ($\varepsilon=4.207\times10^{4}$ $L{\cdot}mol^{-1}{\cdot}cm^{-1}$) because of the stronger D−A effect (Figure S5).

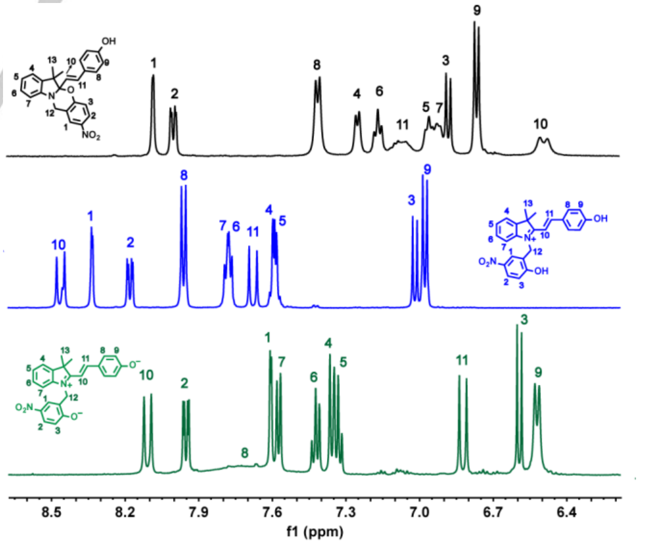

Figure 2. Partial ^1H NMR spectra of M−c (top), M−c with CF_3COOD (M−a−o, middle) and M−c with K_2CO_3 (M−b−o, bottom) in CD_3OD solvent.

NMR measurement to confirm the structures. To demonstrate our conjecture about the structure of three states of M−c molecule (M−c, M−a−o, M−b−o), ^1H NMR spectroscopy measurement was carried out, which is the most powerful method to get the structure information of the organic molecule. The ^{1}H NMR spectra of M−c, M−c with CF_3COOD (M−a−o) and M−c with K_2CO_3 (M−b−o), respectively were obtained in CD_3OD solvent as shown in Figure 2. Compared with ^{1}H NMR spectrum of M−c (black curve), the ^{1}H NMR spectrum after adding acid (blue curve) exhibits obviously downfield shifts overall. The downfield shifts of H4−H11 ascribe to the electron-withdrawing effect of newly generated ammonium cationic. Hereinto, H10 exhibits the largest shift about 1.95 ppm because of the transition of the electron-donating effect of the nitrogen to the electron-withdrawing effect. Furthermore, the slight downfield shift of H1, H2 and H3 declared that the electron density of p-nitrophenol is reduced when a proton is captured. All of these results demonstrate that the M−a−o structure generated after being stimulated by acid.

As for the ^{1}H NMR spectrum of base-form (M−b−o, green curve), H1, H2 and H3 exhibit obviously highfield shift compared with M−c (black curve) and acid-form (M−a−o, blue curve), which indicates that a high-electron-density p-nitrophenol anion is generated. In addition, H8, H9, H10 and H11 exhibit significantly highfield shift compared with M−a−o (blue curve) because the oxygen anion has much stronger electron donor ability. Compared with M−c (black curve), H8 and H10 exhibit downfield shift due to the electron-withdrawing effect of ammonium cationic, while H9 and H11 exhibit highfield shift owing to the electron-donating effect of oxygen anion. Similarly, H4, H5, H6, and H7 exhibit downfield shift comparing with M−c (black curve) due to the electron-withdrawing effect of the adjacent ammonium cationic, and exhibit highfield shift comparing with M−a−o (blue curve) due to the electron-donating effect of oxygen anion on the conjugated structure. All of these phenomena declare that the M−b−o structure generates after being stimulated by the base.

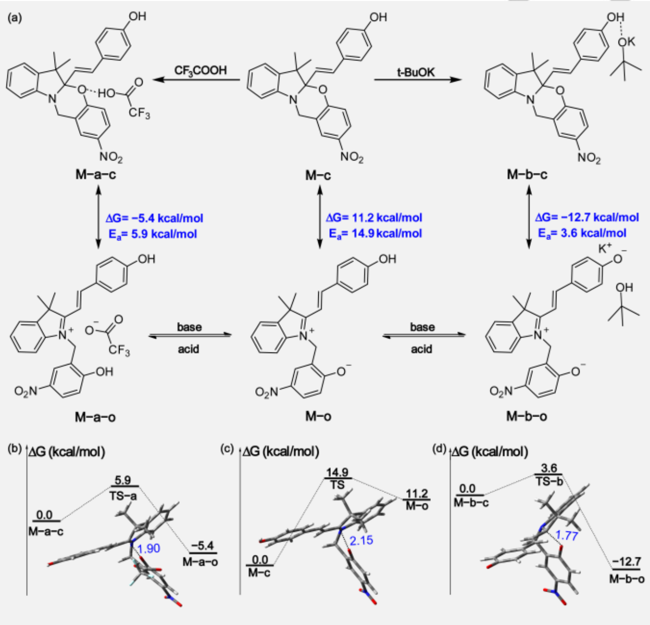

Scheme 1. (a) The switching mechanism of M−c molecule responding to acid and base and the calculated Gibbs Free Energy (ΔG) and Activation Energy (E_a) of different open-ring processes. The calculated energy of the process from (b) M−a−c to M−a−o, (c) M−c to M−o, (d) M−b−c to M−b−o and the structure of transition states.

DFT calculation to speculate switching mechanism. The particularity of M−c molecule is that this molecule has three independent states. The switching mechanism of M−c was speculated as shown in Scheme 1. In the neutral condition, the stable form for M−c molecule is close form, and C−O bond of oxazine may split to obtain the open form M−o. When acid was added, M−c molecule captures proton to form a close form M−a−c firstly, then C−O bond was broken immediately to switch to the open-form M−a−o along with color changing from colorless to yellow. And the proton on the hydroxyl of M−c molecule could be taken away by base to generate a close form M−b−c. Then M−b−c would switch to open-form structure M−b−o with color changing from colorless to red.

DFT calculation method was used to study the mechanism of color changing. The results are shown in Scheme 1. There is only one transition state (TS) in the ring-opening reaction of M−c, in which the bond length of C−O is 2.15 Å. The Gibbs free energy of the ring-opening reaction is about 11.2 kcal/mol which indicates the ring-open process from M−c to M−o is unfavorable in thermodynamic. And activation energy (14.9 kcal/mol is bigger than 10 kcal/mol) also support that the reaction cannot spontaneously take place at room temperature. While for the close-ring process from M−o to M−c, the reaction is great favorable according to the Gibbs free energy (−11.2 kcal/mol) and activation energy (3.7 kcal/mol). The calculated results demonstrate that M−c is more stable than M−o without the environment of acid or base. These agree with the experimental results that the close form M−c is stable state compared by the open form M−o, and once M−o, generated from M−a−o and M−b−o, will switch to close form (M−c) rapidly.

However, after being stimulated by acid and base, the switching direction is converted and the open form is stable state. For the ring-opening process of M−a−c, the bond length of C−O (1.90 Å) of its transition state (TS−a) is shorter than the ring-opening process of M−c. And the open-ring process is much easier for the Gibbs free energy is −5.4 kcal/mol and activation energy is 5.9 kcal/mol. This reaction is unidirectional because the activation energy is 11.3 kcal/mol for the reverse reaction. Which indicates the M−a−o is more stable than M−a−c. For base condition, the transition state (TS−b) has the shortest C−O length (1.77 Å) among these three ring-opening process. The reaction from M−b−c to M−b−o is favorable in thermodynamic according to the Gibbs free energy (−12.7 kcal/mol) and activation energy (3.6 kcal/mol), while the reverse reaction is unfavorable in room temperature according to the activation energy (16.3 kcal/mol). This also indicates the M−b−o is more stable than M−b−c.

Thus, after being stimulated by acid, M−c is switched to M−a−o through M−a−c. Then with being neutralized by base, M−a−o is switched back to M−c through M−o. For being stimulated by base first, and then being neutralized by acid, M−c is switched to M−b−o through M−b−c first, and then M−b−o switches to M−c through M−o. Therefore, the switching under the stimulation of acid and base is unidirectional.

Electrochromic phenomenon and mechanism. The electrochemical properties of M−c were studied through cyclic voltammetry. As shown in Figure 3, the first reductive peak of M−c is at −1.0 V. According to LUMO of M−c calculated by DFT as shown in Figure S6, this peak is supposed to come from the reduction of nitro group of the p-nitrophenol part due to its strong electron-withdrawing property. This speculation is further

10.1002/asia.201800282

confirmed by the similar reductive peak of M−c and p-nitrophenol in Figure 3. The slight difference of reduction peak may come from the difference of C−O and H−O between M−c and p-nitrophenol, and also may come from the spatial electron density influence of the indole part. The reduction state of nitro has alkalinity,[45,46] which may be used to control the M−c base sensitive color change, as we expected.

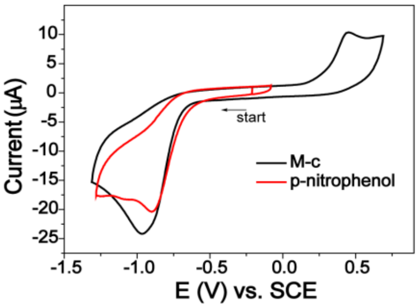

Figure 3. Cyclic voltammograms of M−c (1.0×10^{-3} M) and p-nitrophenol (1.0×10^{-3} M) in acetonitrile with 0.1 M $TBAPF_6$ at scan rate 100 mV/s.

To explore if the M−c molecule has the electro-switchable properties, the changes of absorption spectra during reductive processes were recorded with applying potentials *in situ* as shown in Figure 4a. Before the voltage being applied, the absorption peak is at 267 nm, and there is no absorption in the visible region. After applying a bias voltage (−1.2 V) for 10 s, the absorption peaks at 545 nm, 513 nm and 432 nm emerge and increase with the color changing from colorless to red (Figure 4a, inside photograph). The emerging peaks positions are absolutely same with that of M−b−o obtained by the t-BuOK, which demonstrates that the M−b−o structure can also be obtained by electrical field and M−c molecule exhibits the electro-base property in reductive process. More importantly, the electrochromic behavior of the M−c molecule is reversible. The change of the absorption at 545 nm as the maximum absorption wavelength of M−b−o was monitored *in situ* by UV−vis spectrometers combined with CV as shown in Figure 4b. Before the voltage is applied, there is no absorption at 545 nm. When the M−c began to be reduced at −0.85 V, the absorption at 545 nm began to increase. With the voltage absolute value increasing, the absorption keeps increasing. After the reduced product of M−c began to be oxidized at −0.9 V, the absorption began to decrease until to zero.

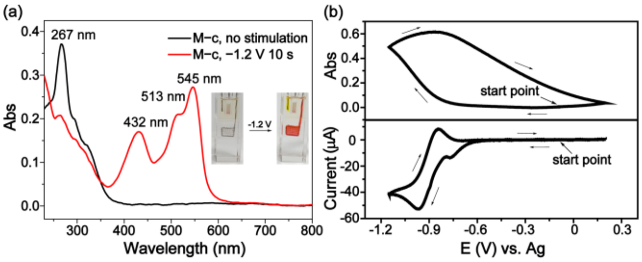

Figure 4. (a) The electrochemical spectra of M−c (1.0×10^{-4} M with 0.1 M $TBAPF_6$ in acetonitrile) under no stimulation and bias voltage at −1.2 V for 10 s measured in situ. (b) Absorption of M−c (1.0×10^{-4} M with 0.1 M $TBAPF_6$ in acetonitrile) changes (top) with the cyclic voltage being applied.

Considering the phenomena and analysis mentioned above, the electro-base mechanism was shown in Scheme 2. Firstly, the M−c molecule was reduced to generate M−r−c with an oxygen anion. The oxygen anion has strong alkalinity which would capture a proton from another M−c molecule to produce the M−r−p, switching another M−c molecule to M−b−o with obvious red color emerging. When the scan direction is reversed, M−r−p is oxidized to M−c−p form. The active proton on nitro of M−c−p go back to the M−b−o, switching the M−b−o to close form M−c. After releasing the proton, the M−c−p turned into the molecule M−c finishing the electro-base cycle. This reversible color changing of switchable molecule base on electro-base mechanism is promising for development a new kind of ECM.

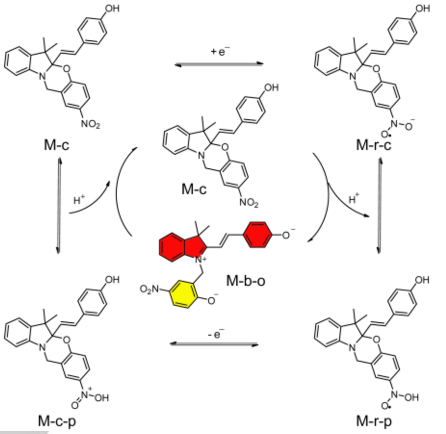

Scheme 2. The mechanism of electrochromic properties of M−c molecule through combining its electro-base property and acid/base sensitive properties.

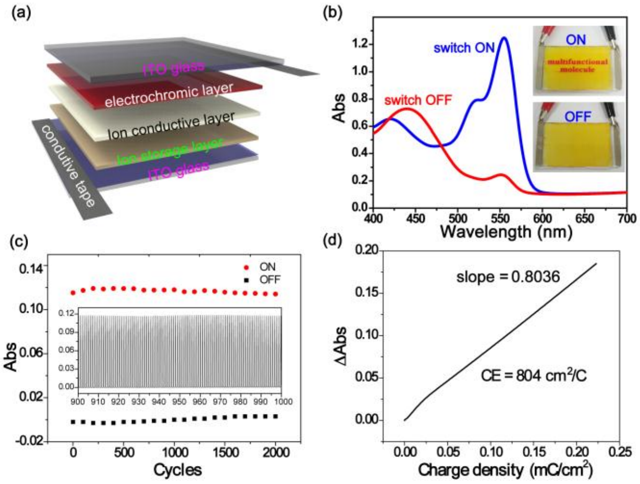

Figure 5. (a) The model of electrochromic device structure. (b) The UV−vis spectra of electrochomic device; (c) Square-wave potential step absorptiometry of electrochromic device (cycle switching time: −1.54 V 600 ms, cut off 0.5 s, then 1 V 4 s, cut off 1 s) and (d) The color efficiency of the electrochromic device. The b, c and d was recorded at 545 nm.

Electrochromic device. To extend the application of the three-states switchable molecules, an electrochromic device was fabricated. The model of this electrochromic device structure was shown in Figure 5a. A thin electrochromic layer and an ion storage layer were separated by an ion conductive layer. The three functional layers were sandwiched between two layers of transparent conducting ITO glasses. The ion conductive layer was used to transport the electrolyte ion and prevent the M−c diffuse to counter layer. In order to balance the charge in the device, ion storage layer containing hydroquinone and benzoquinone was used.

The absorption spectra of the device was recorded by applying a potential *in suit* in Figure 5b. Before being stimulated by bias voltage, the device shows yellow color. After the −1.0 V voltage being applied on the device, the broad absorption peaks at 545 nm, 513 nm appeared with the color changing from yellow to red (blue curve). It is evident that the molecule M−c was switched to M−b−o by electro-base. When a positive voltage (+1.0 V) is applied, the color of the device returns to yellow (red curve) and the peak at 545 nm, 513 nm disappears. The beautiful red text on the device patterned by laser etching method can display reversible stimulated by −1.2 V/1.0 V as shown in the inset picture of Figure 5b. This device is very sensitive to electrical field. The absorption change can be detected by spectrometer even if the stimulating time is as short as 1 millisecond in Figure S7. Furthermore, the reversibility of this device was also monitored. As shown in Figure 5c, no decay of absorption can be seen after 2000 switching cycles. It reveals that this electrochromic device has excellent reversibility and highly durability. In addition, coloration efficiency is an important index to evaluate the electron efficiency of electrochromic device. Herein, coloration efficiency was estimated to be as high as 804 cm^2/C, which is extremely high compared with traditional small molecule and metal oxide electrochromic device (Figure 5d). These measurements declare that the multifunctional M−c molecule can be used to fabricate high performance electrochromic devices.

Conclusions

A multi-functional molecular switch M−c with excellent acid and base sensitive properties was designed and synthesized. Structures of its respective three states, neutral-form M−c, acid-form M−a−o and base-form M−b−o, were speculated by comparing the absorption spectra with reference molecules and proved by NMR. The structure changing mechanism of M−c under the stimulation of acid/base was analyzed by DFT calculation. This multi-function switchable molecule can be used not only as an acid/base indicator, but as electro-base. An electrochromic device based on electro-base and acid/base responsive properties was successfully fabricated. Color switching between red and yellow can be controlled by altering voltages. The device exhibits good properties with good reversibility (2000 cycles) and high coloration efficiency (804 cm^2/C). This successful attempt for using molecular switches as electrochromic material provides a novel thoughts for the creation of new electrochromic devices and other display devices.

Experimental Section

Materials

Acetonitrile (chromatographic grade), tetrabutylammonium hexafluorophosphate (TBAPF$_6$), trifluoroacetic acid (TFA) and potassium tert-butoxide (t-BuOK) were purchased from Aladdin Reagent Company (Shanghai, China). Polymethyl methacrylate (PMMA), propylene carbonate (PC), p-benzoquinone, p-hydroquinone, p-nitrophenol, p-anisaldehyde and p-hydroxybenzaldehyde were purchased from Energy Chemical Company (Shanghai, China). TBAPF$_6$ was recrystallized three times from ethanol and dried under vacuum at 80˚C prior to use. Other chemicals (analytical grade) were used as received without further purification.

Preparation of Electrochromic device

First, a solution for fabricating electrochromic layer was prepared by dissolving 0.36 g of PMMA, 0.075 ml of PC, 0.15 g of TBAPF$_6$ and 8.29 mg of M−c molecules in 2 ml of acetonitrile. A solution for fabricating ion storage layer was prepared by dissolving 0.9 g of PMMA, 0.187 ml of PC, 0.375 g of TBAPF$_6$, 54 mg of p-benzoquinone and 110 mg of hydroquinone in 10 ml of acetonitrile. A solution to make conductive layer was prepared by dissolving 3.6 g of PMMA, 0.75 ml of PC and 1.5 g of TBAPF$_6$ in 20 ml of acetonitrile. The mixtures were stirred for 5 h at 40 ˚C. Three homogeneous and transparent solutions were obtained. The electrochromic layer and the ion storage layer were respectively dropcasted on two ITO glasses. After drying at room temperature for the ion storage layer, a layer of conductive layer was dropcasted on the top. After the solvent was evaporated, the two ITO glasses were clamped together that the following a transparent electrochromic device with symmetrically layered was obtained.

Synthesis of M−c and M−r−1 and M−r−2

M−c was prepared through the following procedures[48]: 5a,6,6-trimethyl-2-nitro-5a,6-dihydro-12H-benzo[5,6][1,3]oxazino[3,2-a]indole (SM1) (1.6 mmol, 496 mg) and p-hydroxybenzaldehyde (2.2 mmol, 268 mg) were heated and refluxed in 25 ml ethanol solution for 8 h under argon atmosphere. After cooling to ambient temperature, the solvent was removed with rotary vacuum evaporator and treated with NaHCO$_3$ aqueous solution. Acetic ether was added to extract the product and dried with anhydrous sodium sulfate. The solvent was distilled off under reduced pressure. The residual solid was purified by flash chromatography (petroleum ether/ethyl acetate = 5:1) to obtain a red solid powder(412 mg, 62%). ^{1}H NMR (500 MHz, DMSO) δ = 9.63 (s, 1H), 8.13 (s, 1H), 8.02 – 7.91 (m, 1H), 7.36 (d, *J* = 8.2 Hz, 2H), 7.18 (d, *J* = 7.1 Hz, 1H), 7.07 (t, 1H), 6.96 (d, *J* = 9.1 Hz, 1H), 6.84 (d, *J* = 7.8 Hz, 1H), 6.81 (t, 1H), 6.72 (d, *J* = 8.1 Hz, 3H), 6.30 (d, *J* = 16.1 Hz, 1H), 4.74 (s, 2H), 1.32 (s, 6H). ^{13}C NMR (126 MHz, DMSO) δ = 159.55, 158.46, 147.03, 140.35, 138.32, 135.74, 128.97, 127.94, 126.89, 124.20, 124.08, 122.67, 121.28, 120.75, 118.03, 115.94, 109.48, 104.77, 49.92, 49.07, 23.57, 22.50. LC-HRMS: m/z [M+H]$^+$ calculated for 415.1652, found 415.1649. Melting point: 153.1−153.9 ˚C.

M−r−1 was synthesized through the following procedures : 5a,6,6-trimethyl-2-nitro-5a,6-dihydro-12H-benzo[5,6][1,3]oxazino[3,2-a]indole (SM1) (1 mmol, 310 mg), p-anisaldehyde (2 mmol, 272 mg) and methanesulfonic acid (1.5 mmol, 144 mg) was heated and refluxed at 10 ml ethanol solution for 4 h under argon atmosphere. After cooling to ambient temperature, the solvent was removed with rotary vacuum evaporator and treated with NaHCO$_3$ aqueous solution. Acetic ether was added to extract the product and dried with anhydrous sodium sulfate. The solvent was distilled off under reduced pressure. The crude product was precipitate through adding n-hexane to acetic ether. And the crude product was further purified by flash chromatography (petroleum ether/ethyl acetate = 3:1 with 0.5 % volume fraction of triethylamine) to obtain a white solid powder (351 mg, 82%). ^{1}H NMR (500 MHz, CDCl3) δ 8.00 (s, 1H), 7.97 (d, J = 9.0 Hz, 1H), 7.34 (d, J = 8.5 Hz, 2H), 7.16 – 7.07 (m, 2H), 6.86 (d, J = 8.7 Hz, 4H), 6.74 (d, J = 16.1 Hz, 1H), 6.61 (d, J = 7.8 Hz, 1H), 6.20 (d, J = 16.1 Hz, 1H), 4.58 (s, 2H), 3.80 (s, 3H), 1.37 (s, 6H). ^{13}C NMR (126 MHz, CDCl3) δ 160.10, 159.42, 146.58, 140.70, 138.36, 135.65, 128.45, 128.26, 127.73, 124.07, 123.33, 122.42, 121.54, 120.77, 120.15, 117.75, 114.24, 108.86, 104.02, 55.47, 50.12, 40.79, 26.61, 18.73. LC-HRMS: m/z calculated for $C_{26}H_{24}N_2O_4$ 429.1809, found 429.1801. Melting point: 168.2−169.0 ˚C.

M−r−2 was synthesized according to the following procedures: the solution of 1,2,3,3-tetramethyl-3H-indol-1-ium iodide (1 mmol, 301 mg) and p-hydroxybenzaldehyde (1.2 mmol, 146 mg) in 10 ml ethanol was refluxed for 6 h. The solvent was removed with rotary vacuum evaporator. The crude product was washed by acetic ether to get red solid powder (348 mg, 86%). ^{1}H NMR (500 MHz, DMSO) δ 10.81 (s, 1H), 8.36 (d, J = 16.2 Hz, 1H), 8.13 (d, J = 8.5 Hz, 2H), 7.87 – 7.81 (m, 2H), 7.61 (t, J = 7.0 Hz, 1H), 7.60 – 7.55 (t, J = 7.0 Hz, 1H), 7.46 (d, J = 16.2 Hz, 1H), 6.96 (d, J = 8.7 Hz, 2H), 4.08 (s, 3H), 1.77 (s, 6H).

DFT Calculation

The quantum chemical calculations were performed with the Gaussian 09 program.[48] The geometries of all the molecules, molecular transition states and their energy were optimized (in vacuum) and calculated by the density functional theory (DFT) method by using RB3LYP/ 6−31+G (d). Frequency calculations were carried out to confirm the local minima possess all real frequencies.

Acknowledgements

This study was supported by the National Science Foundation of China (Grant No. 21602075, 21572079) and the program for JLU Science and Technology Innovative Research Team (JLUSTIRT).

Conflict of Interest

The authors declare no conflict of interest.

Keywords: molecular switch • oxazine• base sensitive • electro-base • electrochromic material

[1] R. J. Mortimer, *Annu. Rev. Mater. Res.* **2011**, 41, 241-268.

[2] P. R. Somani and S. Radhakrishnan, *Mater. Chem. Phys.* **2003**, 77, 117-133.

[3] C. M. Lampert, *Mater. Today* **2004**, 7, 28-35.

[4] R. Baetens, B. P. Jelle and A. Gustavsen, *Sol. Energy Mater. Sol. Cells* **2010**, 94, 87-105.

[5] C. G. Granqvist, *Thin Solid Films* **2014**, 564, 1-38.

[6] J. L. Wang, Y. R. Lu, H. H. Li, J. W. Liu and S. H. Yu, *J. Am. Chem. Soc.* **2017**, 139, 9921-9926.

[7] G. Cai, P. Darmawan, X. Cheng and P. S. Lee, *Adv. Energy Mater.* **2017**, 7, 1602598.

[8] L. Xiao, Y. Lv, J. Lin, Y. Hu, W. Dong, X. Guo, Y. Fan, N. Zhang, J. Zhao, Y. Wang and X. Liu, *Adv. Opt. Mater.* **2018**, 6, 1700791.

[9] R. J. Mortimer, A. L. Dyer and J. R. Reynolds, *Displays* **2006**, 27, 2-18.

[10] S. Mishra, P. Yogi, S. K. Saxena, S. Roy, P. R. Sagdeo and R. Kumar, *J. Mater. Chem. C* **2017**, 5, 9504-9512.

[11] G. Cai, J. Wang and P. S. Lee, *Acc. Chem. Res.* **2016**, 49, 1469-1476.

[12] L. Beverina, G. A. Pagani and M. Sassi, *Chem. Commun.* **2014**, 50, 5413-5430.

[13] P. M. Beaujuge and J. R. Reynolds, *Chem. Rev.* **2010**, 110, 268-320.

[14] P. M. Beaujuge, S. Ellinger and J. R. Reynolds, *Nat. Mater.* **2008**, 7, 795-799.

[15] L. Striepe and T. Baumgartner, *Chem. Eur. J.* **2017**, 23, 16924-16940.

[16] D. T. Gillaspie, R. C. Tenent and A. C. Dillon, *J. Mater. Chem. C* **2010**, 20, 9585.

[17] P. Jia, A. A. Argun, J. Xu, S. Xiong, J. Ma, P. T. Hammond and X. Lu, *Chem. Mater.* **2010**, 22, 6085-6091.

[18] V. K. Thakur, G. Ding, J. Ma, P. S. Lee and X. Lu, *Adv. Mater.* **2012**, 24, 4071-4096.

[19] Q. Liu, Q. Chen, Q. Zhang, Y. Xiao, X. Zhong, G. Dong, M. P. Delplancke-Ogletree, H. Terryn, K. Baert, F. Reniers and X. Diao, *J. Mater. Chem. C*, **2018**, 6, 646-653.

[20] S. Guan, A. S. Elmezayyen, F. Zhang, J. Zheng and C. Xu, *J. Mater. Chem. C* **2016**, 4, 4584-4591.

[21] S. Shankar, M. Lahav and M. E. van der Boom, *J. Am. Chem. Soc.* **2015**, 137, 4050-4053.

[22] H. Y. Qu, D. Primetzhofer, M. A. Arvizu, Z. Qiu, U. Cindemir, C. G. Granqvist and G. A. Niklasson, *ACS Appl. Mater. Interfaces* **2017**, 9, 42420-42424.

[23] G. Luo, L. Shen, J. Zheng and C. Xu, *J. Mater. Chem. C* **2017**, 5, 3488-3494.

[24] G. Luo, K. Shen, J. Zheng and C. Xu, *J. Mater. Chem. C* **2016**, 4, 9085-9093.

[25] B. Gelinas, D. Das and D. Rochefort, *ACS Appl. Mater. Interfaces* **2017**, 9, 28726-28736.

[26] N. Elool Dov, S. Shankar, D. Cohen, T. Bendikov, K. Rechav, L. J. W. Shimon, M. Lahav and M. E. van der Boom, *J. Am. Chem. Soc.* **2017**, 139, 11471-11481.

[27] J. T. S. Allan, S. Quaranta, Ebralidze, II, J. G. Egan, J. Poisson, N. O. Laschuk, F. Gaspari, E. B. Easton and O. V. Zenkina, *ACS Appl. Mater. Interfaces*, **2017**, 9, 40438-40445.

[28] Y. Tian, W. Zhang, S. Cong, Y. Zheng, F. Geng and Z. Zhao, *Adv. Funct. Mater.* **2015**, 25, 5833-5839.

[29] J. Sun, Y. Dai, M. Ouyang, Y. Zhang, L. Zhan and C. Zhang, *J. Mater. Chem. C* **2015**, 3, 3356-3363.

[30] Y. Ling, C. Xiang and G. Zhou, *J. Mater. Chem. C* **2017**, 5, 290-300.

[31] J. Sun, X. Lv, P. Wang, Y. Zhang, Y. Dai, Q. Wu, M. Ouyang and C. Zhang, *J. Mater. Chem. C* **2014**, 2, 5365.

[32] L. He, G. Wang, Q. Tang, X. Fu and C. Gong, *J. Mater. Chem. C* **2014**, 2, 8162-8169.

[33] D. C. Huang, J. T. Wu, Y. Z. Fan and G. S. Liou, *J. Mater. Chem. C* **2017**, 5, 9370-9375.

[34] S. Swaminathan, J. Garcia-Amoros, E. R. Thapaliya, S. Nonell, B. Captain and F. M. Raymo, *ChemPhysChem* **2016**, 17, 1852-1859.

[35] Y. Wang, X. Tan, Y. M. Zhang, S. Zhu, I. Zhang, B. Yu, K. Wang, B. Yang, M. Li, B. Zou and S. X. Zhang, *J. Am. Chem. Soc.* **2015**, 137, 931-939.

[36] K. Redeckas, V. Voiciuk, R. Steponaviciute, V. Martynaitis, A. Sackus and M. Vengris, *J. Phys. Chem. A* **2014**, 118, 5642-5651.

[37] E. Deniz, M. Tomasulo, J. Cusido, S. Sortino and F. M. Raymo, *Langmuir* **2011**, 27, 11773-11783.

[38] M. Tomasulo, S. Sortino, A. J. White and F. M. Raymo, *J. Org. Chem.* **2005**, 70, 8180-8189.

[39] Y. Zhang, S. Tang, L. Sansalone, J. D. Baker and F. M. Raymo, *Chem. Eur. J.* **2016**, 22, 15027-15034.

[40] S. Impellizzeri, S. Simoncelli, G. K. Hodgson, A. E. Lanterna, C. D. McTiernan, F. M. Raymo, P. F. Aramendia and J. C. Scaiano, *Chem. Eur. J.* **2016**, 22, 7281-7287.

[41] E. Deniz, M. Tomasulo, J. Cusido, I. Yildiz, M. Petriella, M. L. Bossi, S. Sortino and F. M. Raymo, *J. Phys. Chem. C* **2012**, 116, 6058-6068.

[42] P. Beaujean, F. Bondu, A. Plaquet, J. Garcia-Amoros, J. Cusido, F. M. Raymo, F. Castet, V. Rodriguez and B. Champagne, *J. Am. Chem. Soc.* **2016**, 138, 5052-5062.

[43] S. Zhu, M. Li, S. Tang, Y. M. Zhang, B. Yang and S. X. A. Zhang, *Eur. J. Org. Chem.* **2014**, 1227-1235.

[44] E. Deniz, S. Impellizzeri, S. Sortino and F. M. Raymo, *Can. J. Chem.* **2011**, 89, 110-116.

[45] Y. M. Zhang, M. Li, W. Li, Z. Huang, S. Zhu, B. Yang, X. C. Wang and S. X. A. Zhang, *J. Mater. Chem. C* **2013**, 1, 5309.

[46] Y. M. Zhang, X. Wang, W. Zhang, W. Li, X. Fang, B. Yang, M. Li and S. X. A. Zhang, *Light: Sci. Appl.* **2015**, 4, e249.

[47] X. Wang, W. Li, W. Li, C. Gu, H. Zheng, Y. Wang, Y. M. Zhang, M. Li and S. Xiao An Zhang, *Chem. Commun.* **2017**, 53, 11209-11212.

[48] M. J. Frisch, G. W. Trucks, H. B. Schlegel, G. E. Scuseria, M. A. Robb, J. R. Cheeseman, G. Scalmani, V. Barone, B. Mennucci, G. A. Petersson, H. Nakatsuji, M. Caricato, X. Li, H. P. Hratchian, A. F. Izmaylov, J. Bloino, G. Zheng, J. L. Sonnenberg, M. Hada, M. Ehara, K. Toyota, R. Fukuda, J. Hasegawa, M. Ishida, T. Nakajima, Y. Honda, O.

Kitao, H. Nakai, T. Vreven, J. A. Jr. Montgomery, J. E. Peralta, F. Ogliaro, M. Bearpark, J. J. Heyd, E. Brothers, K. N. Kudin, V. N. Staroverov, R. Kobayashi, J. Normand, K. Raghavachari, A. Rendell, J. C. Burant, S. S. Iyengar, J. Tomasi, M. Cossi, N. Rega, J. M. Millam, M. Klene, J. E. Knox, J. B. Cross, V. Bakken, C. Adamo, J. Jaramillo, R. Gomperts, R. E. Stratmann, O. Yazyev, A. J. Austin, R. Cammi, C. Pomelli, J. W. Ochterski, R. L. Martin, K. Morokuma, V. G. Zakrzewski, G. A. Voth, P. Salvador, J. J. Dannenberg, S. Dapprich, A. D. Daniels, O. Farkas, J. B. Foresman, J. V. Ortiz, J. Cioslowski, D. J. Fox, Gaussian 09, (Revision A. 02), Gaussian, Inc., Wallingford, CT, **2009**.

10.1002/asia.201800282

Entry for the Table of Contents (Please choose one layout)

Layout 1:

FULL PAPER

Multifunctional molecular switch: By endowing the electro-base property and acid/base responsive properties with oxazine molecular switch, a new kind of electrochromic material with great performance was successfully fabricated.

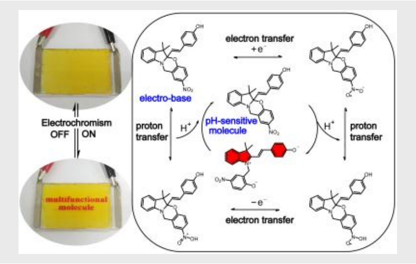

New-type Electrochromic Material

Xiaojun Wang, Chang Gu, Hongzhi Zheng, Yu-Mo Zhang, Sean Xiao-An Zhang**

Page No. – Page No.

A multi-stimuli-responsive oxazine molecular switch: A new strategy for the design of electrochromic materials

For internal use, please do not delete. Submitted_Manuscript